Minimum non-isotropic and asymmetric margins for taking into account intrafraction prostate motion during moderately hypofractionated radiotherapy

Francesca Di Franco, Thomas Baudier, Frédéric Gassa, Alexandre Munoz, Murielle Martinon, Sarah Charcosset, Emilie Vigier-Lafosse, Pascal Pommier, David Sarrut, Marie-Claude Biston

Minimum non-isotropic and asymmetric margins for taking into account intrafraction prostate motion during moderately hypofractionated radiotherapy

Francesca di Franco[1,2], Thomas Baudier[1,2], Frédéric Gassa[1], Alexandre Munoz[1], Murielle Martinon[1], Sarah Charcosset[1], Emilie Vigier-Lafosse[1], Pascal Pommier[1], David Sarrut[1,2] and Marie-Claude Biston[1,2,*]

[1] Centre Léon Bérard, 28 rue Laennec 69373, LYON Cedex 08, France

[2] CREATIS, CNRS UMR5220, Inserm U1044, INSA-Lyon, Université Lyon 1, Villeurbanne, France

*Corresponding author. Department of Radiation Oncology, Centre Léon Bérard, 28 rue Laennec, 69373 Lyon Cedex 08, France

E-mail address: marie-claude.biston@lyon.unicancer.fr

Abstract:

Purpose: To investigate the impact on dose distribution of intrafraction motion during moderate hypofractionated prostate cancer treatments and to estimate minimum non-isotropic and asymmetric (NI-AS) treatment margins taking motion into account.

Methods: Prostate intrafraction 3D displacements were recorded with a transperineal ultrasound probe and were evaluated in 46 prostate cancer patients (876 fractions) treated by moderate hypofractionated radiation therapy (60Gy in 20 fractions). For 18 patients (346 fractions), treatment plans were recomputed increasing CTV-to-PTV margins from 0 to 6mm with an auto-planning optimization algorithm. Dose distribution was estimated using the voxel shifting method by displacing CTV structure according to the retrieved movements. Time-dependent margins were finally calculated using both van Herk's formula and the voxel shifting method.

Results: Mean intrafraction prostate displacements observed were -0.02±0.52mm, 0.27±0.78mm and -0.43±1.06mm in left-right, supero-inferior and antero-posterior directions, respectively. The CTV dosimetric coverage increased with increased CTV-to-PTV margins but it decreased with time. Hence using van Herk's formula, after 7min of treatment, a margin of 0.4 and 0.5mm was needed in left and right, 1.5 and 0.7mm in inferior and superior and 1.1 and 3.2mm in anterior and posterior directions, respectively. Conversely, using the voxel shifting method, a margin of 0mm was needed in left-right, 2mm in superior, 3mm in inferior and anterior and 5mm in posterior directions, respectively. With this latter NI-AS margin strategy, the dosimetric target coverage was equivalent to the one obtained with a 5mm homogeneous margin.

Conclusions: NI-AS margins would be required to optimally take into account intrafraction motion.

Keywords: Prostate cancer, Hypofractionation, Intrafraction motion, Margins.

Introduction

Hypofractionated (HF) radiation therapy protocols have shown their effectiveness in treating prostate cancer patients (1, 2). However, these protocols require a high level of accuracy in dose delivery to allow reducing treatment margins because of an increased risk of toxicity to the surrounding organs at risk (OARs) (3). The use of reduced clinical target volume to planning target volume (CTV-to-PTV) margins for HF versus conventional fractionated treatments has shown to lead to similar late effects between the 2 cohorts (4) whereas early side effects were more pronounced for HF treatments (4). Using a monitoring device to control intrafraction prostate motion would enable to further reduce HF treatment margins, thus decreasing the risk of early side toxicity (5).

The effect of geometric uncertainties is known to be one of the major concerns in prostate cancer. These are generally due to rectum and bladder motion, which has been shown to be correlated to their fullness (6). Prostate motion can be important (displacements > 1 cm) but also irregular and sometimes unpredictable (7). Many authors have already studied the magnitude of prostate shifts occurred during treatment fractions, using different prostate monitoring devices (8-12). Thus, using the Calypso system (Varian Medical Systems, Palo Alto, CA) to monitor prostate motion, *Langen et al*. (9) reported that displacements > 3 mm could be observed 5 min after alignment. Using a transperineal ultrasound (TP-US) probe (Clarity®, Elekta AB, Stockholm, Sweden) for monitoring prostate displacement, *Baker et al.* (10) observed deviations up to 2.8 mm after only 2.5 min of treatment, and *Sihono et al.* observed displacements of more than 6 mm after 4 minutes of treatment (11). Magnetic resonance-linac technology is also very accurate in retrieving prostate intrafraction motion, but little available due to its high cost compared to other technologies. Using this technology *de Muinck Keizer et al.* (13) also reported important displacements (>4 mm in posterior and superior directions) after 6 minutes of treatment time.

While the shifts observed are likely to have little impact on dose distribution if the treatment is delivered with a high number of fractions, this is not true for HF treatments (14, 15). Besides, during HF treatments, because of an increased risk of toxicity to the surrounding organs, CTV-to-PTV margins should be reduced compared to conventional treatments, which seems difficult in the absence of monitoring systems. Therefore, a finer determination of the planning target volume (PTV) margin is crucial for safe dose escalation. Consequently an adapted margins strategy is needed. The most used method to estimate the required CTV-to-PTV margins is the van Herk's formula (16). Several assumptions and simplifications have been used for this approach to be valid (16): patient population was assumed to be homogeneous (same standard deviations' values were assumed for each patient) and many fractions were

considered in order to put treatment average execution error as zero. Those simplifications cannot be ignored in presence of a heterogeneous population, where large random variations occur, or in presence of a reduced number of fractions (14). In addition, margins recipes only take into account interfraction motion with few guidelines for intrafraction movements (17). Thus, other alternatives must be explored in order to accurately estimate treatment margins for taking into account intrafraction movements.

Another method which could be more relevant is the voxel shifting method. It consists in shifting the dose map according to translations or rotations observed during the treatment process. This way, the effect of movements on the dose distribution is directly visible, which makes it possible to extract a margin taking into account the movements on a patient population. This method is particularly relevant for photon treatment, since the photon range is little disturbed by a change in patient anatomy, which enabled the dose distribution to be calculated using the static dose cloud approximation (18). This method appears all the more appropriate when used in a homogeneous environment as it is the case for prostate cancer (18).

Hence, the goal of this work was to propose a population-based study to retrieve non-isotropic and asymmetric (NI-AS) CTV-to-PTV minimum margins only taking into account intrafractional prostate motion. Forty-six patients (876 fraction) having received moderate HF prostate treatment (60 Gy in 20 fractions) and daily monitored using Clarity TP-US probe were considered in this study. The retrieved displacements were used to study the CTV-target coverage during treatment, in presence of motion. The CTV structure was perturbed with the recorded prostate displacements using the voxel shifting method and the static dose cloud approximation (18). Then, to evaluate the effectiveness of NI-AS margins, treatment plans were re-computed using an autoplanning algorithm (19). Several studies dealing with intrafraction prostate monitoring during treatment can be found in the literature (9-11, 20) as well as many margins recipes that consider interfractional motion (16, 17, 21). However, to our knowledge, this is one of the first that uses monitoring device to investigate non homogeneous and time-dependent margins for intrafractional prostate motion during moderate HF radiation therapy. An ulterior novel feature proposed by this work is the use of an automatic treatment plan algorithm that enabled assessing the impact of intrafraction motion on CTV coverage without having operator variability in the planning process which could bias the conclusions.

Materials and methods

TP-US monitoring device

The Clarity 3D TP-US system is based on a 2D TP-US probe tracked by an infrared camera (22). For each acquisition, hundreds of 2D US slices are acquired during an automated probe sweeping movement performed by a step-by-step motor and merged into a 3D image. The probe can complete a 75° sweep in 0.5 seconds and the patient does not perceive any motion other than a slight vibration, as all motion is internal to the probe housing. For patients' positioning, a specific immobilization device made of a base plate and 2 cushions for the knees enables the probe to be fixed between patient's legs. During the planning CT session, an US reference image (US_{ref}) is acquired with the patient in the same position as during the CT acquisition. The US_{ref} image is superimposed to the CT image through a calibration process, allowing the visualization of the US_{ref} and CT images in the same coordinates system. A reference positioning volume (RPV) is then delineated on the US_{ref} image. During the treatment course, a daily US image (US_{daily}) is acquired at the beginning of each fraction and manually registered on the US_{ref} image by RPV projection. The monitoring is performed via continuous 3D automatic rigid registration of the current US image with the US_{daily} image (0.7 s for each registration).

Patients' cohort and clinical protocol

Forty-six patients receiving a moderate HF volumetric modulated arc therapy (VMAT) treatment of the prostate in our institution were included in this study, which was approved by the hospital ethics committee. The prescribed dose was 60 Gy in 20 fractions delivered to the PTV. A dose objective was fixed for CTV: 99% of the CTV covered by 100% of the prescribed dose. VMAT treatments were delivered using a VersaHD® (Elekta AB) Linac. Before the treatment, a US_{daily} image followed by a Cone Beam CT (CBCT) acquisition was performed for pretreatment positioning. The CBCT was the reference modality for patient positioning whereas the TP-US probe was only used for controlling intrafraction motion of the prostate (876 fractions). Treatment durations ranged between 200-600 s. Among the cohort, 18 patients (346 fractions) were randomly selected for treatment plan re-computation using increased CTV-to-PTV margins (i.e., 0, 1, 2, 3, 4, 5 and 6 mm margins around the CTV). Patients followed an individual bladder preparation of 1–2 cups of water (330–500 ml) 1 hour before the treatment. Specific dietary advices were given for a period of 7 days before the CT scanner. Patients were also encouraged to empty their bowels and bladder prior to each fraction.

Treatment planning

One hundred and forty four VMAT treatment plans were re-computed using increased CTV-to-PTV margins with mCycle auto-planning solution, which is implemented in a research version of Monaco TPS (V.5.59.11, Elekta AB, Stockholm). This concept, using lexicographic Multi Criteria Optimization (MCO) has been extensively described before (19). To summarize, the first step is defining a "tumor and protocol" specific wish-list containing the constraints and prioritized objectives. Then through the optimization process, firstly the algorithm is optimizing the individual objectives to meet the different requested goal values and all defined constraints while respecting the priority order. Then it tries to further reduce the objectives that were below the goal value in the first pass, as low as possible in a second pass. All plans were performed using the same beam geometry (two 360° arcs), the same wish-list, and the same sequencing parameters to avoid any bias in dosimetric comparisons related to the planning process.

Quantification of the impact of intrafraction motion on target coverage

The robustness of a treatment plan was evaluated by performing transformations of the nominal dose distribution and estimating differences. The voxel shifting method (18) and the static dose cloud approximation were used to move the CTV RT structure with the prostatic displacements observed during the treatment process. An in-house automated Python routine was developed to take as input the planning CT, RT structures and 3D displacements of the prostate (left-right (LR), superior-inferior (SI) and anterior-posterior (AP)) and generate as output the moved structures. Hence, the RT structures were moved each 5 seconds according to the given displacements. The 60 Gy isodoses RT structures were retrieved from the calculated plans using different CTV-to-PTV margins, and then superimposed onto the moved CTV to verify the dosimetric coverage. This way, the theoretical coverage of the CTV was evaluated each 5 seconds, in presence of motion.

Margin's analysis (statistical analysis)

As reported elsewhere (17, 21), the van Herk's non-linear margin recipe (16) was used to estimate the duration-dependent margins for every minute up to

10 min as followed:

$$M = \left(C_1 \Sigma + C_2 \left(\sqrt{\sigma^2 + \sigma_p^2} - \sigma_p \right) \right) \qquad (1)$$

As defined by *van Herk* (23) Σ is the standard deviation of the mean displacements (systematic errors) and σ is the standard deviation of the random variations (prostate motion). The parameter σ_p (3.2 mm) describes the width of the penumbra modeled by a cumulative Gaussian.

C_1 is the confidence level corresponding to a percentage of the population and C_2 is the dose level's coefficient. C_1 and C_2 were chosen to achieve the two following dosimetric criteria: 90% of population which CTV was covered by 95% of total dose (90PP-95D) and 95% of population having the CTV covered by 99% of the total dose (95PP-99D). For the 90PP-95D dosimetric criteria, C_1 and C_2 values were chosen as 2.50 and 1.64, respectively. Instead, for 95PP-99D dosimetric criteria, C_1 and C_2 values were set as 2.79 and 2.34, respectively (16). Whereas the first criterion was the one used by *van Herk* (16) and largely reported in literature, the second one was chosen to better consider the specific conditions relating to HF treatments (reduced number of fractions and higher treatment accuracy needed).

Results

Motion analysis

The evaluation of 876 fractions after 5 min of treatment resulted in a mean displacement of -0.02 ± 0.52 mm, 0.27 ± 0.78 mm and -0.43 ± 1.06 mm in the LR, SI and AP directions respectively. After 10 min of treatment mean displacements were -0.03 ± 0.76 mm, 0.45 ± 1.08 mm and -0.72 ± 1.50 mm. To visualize the data over all the fractions, 425 104 displacement values were plotted in a histogram (Fig. 1). Mean absolute displacements > 3, 5 and 7 mm were observed for 16%, 5%, and 2% of the total number of fractions. Rare large deviations > 8 mm were detected but the frequency was less than 1%. On average, the evaluation of the trajectories revealed a directional dependence of the intrafractional prostate movements. The prostate position was rather stable in LR direction, with median and maximum values of -0.02 and 7.60 mm after 10 min of treatment. In contrast, the evaluation in SI and AP directions showed a wider variation of displacements values (standard deviation of 1.08 and 1.50 mm after 10 min treatment respectively). Prostate movements were

more important in inferior and posterior directions, with median values of 0.28 and -0.50 mm and maximum values of 9.54 and 9.50 mm after 10 min of treatment, respectively.

CTV coverage study using homogeneous margins

Isotropic margins of 0, 1, 2, 3, 4, 5 and 6 mm were added to each pre-treatment CTV structure and, after applying the registered 3D shifts, the corresponding shifted CTV covered by 60 Gy isodose RT structure was recorded each 5 seconds from 0 to 600 s for each CTV-to-PTV margin value. The median CTV dosimetric coverage obtained depending on time, using the above mentioned CTV-to-PTV margins is shown in Fig.2. The CTV coverage increased with increased CTV-to-PTV margins but it decreased with time. Median shifted dose distribution results showed that, fixing 300 s as observation time and considering 330 fractions, the prescription constraint (99% of the CTV covered by 100% of the prescribed dose) on the CTV was achieved in 77%, 77%, 78%, 84%, 92%, 98% and 100% of fractions using 0, 1, 2, 3, 4, 5 and 6 mm margins, respectively. Considering that the average duration of a HF treatment is about 5 min, a homogeneous margin of 5 mm was considered as sufficient to take into account intrafraction motion. Then, considering that the prostate can move during the imaging and pretreatment verification phase, the observation time was increased to 7 and 10 min, corresponding to a 2 and 5 min imaging phase, respectively. In the first case, fixing 420 s as observation time (277 fractions) the prescription constraint on CTV prostate was achieved in 71%, 71%, 72%, 85%, 89%, 95% and 98% of fractions using 0, 1, 2, 3, 4, 5 and 6 mm margins, respectively. Alternatively, fixing 600 s as observation time (97 fractions) the prescription constraint on CTV prostate was achieved in 67%, 68%, 69%, 69%, 70%, 85% and 95% of fractions using 0, 1, 2, 3, 4, 5 and 6 mm margins, respectively. Hence, after 7 min total treatment time, a homogeneous margin of 5 mm should guarantee a correct prostate target coverage, whereas 10 min total treatment time, would require a 6 mm CTV-to-PTV margin.

Treatment margins

Based on the data acquired in this study (46 patients, 876 fractions), time-dependent margins were calculated to account for intrafraction motion. Non-

isotropic margins were first calculated using van Herk's formula. To meet the first 90PP-95D dosimetric criterion after 10min of treatment, margins of 1.5, 3.2 and 6.2 mm were calculated in LR, SI and AP directions, respectively. In order to meet the targeted dosimetry criterion of 95PP-99D, the margin was increased by 0.2, 0.5 and 1 mm, in the LR, SI and AP directions, respectively (Table 1).

Since the evaluation of the trajectories revealed a directional dependence of the intrafraction prostate motion, with important displacements in inferior and posterior directions, NI-AS and time-dependent margins were first calculated using the van Herk's formula and then retrieved using the voxel shifting method. Hence, after 10 min of treatment, using van Herk's formula, a margin of 0.5 and 0.6 mm was needed in left and right directions, respectively, 1.7 and 0.7 mm in inferior and superior, respectively, and 0.9 and 3.5 mm in anterior and posterior directions, respectively, to meet the 90PP-95D dosimetric criterion (Table 1). To achieve the targeted criterion of 95PP-99D, after 10 min of treatment, a margin of 0.5 and 0.7 mm was needed in left and right directions, respectively, 1.9 and 0.8 mm in inferior and superior directions, respectively and 1.1 and 4.6 in anterior and posterior directions, respectively.

Using the voxel shifting method, margins needed to meet the 95PP-99D dosimetric criterion were generally more important, except in left-right direction. Hence, after 10 min of treatment, a margin of 0 and 1 mm was needed in left and right directions, respectively, 4 and 3 mm in inferior and superior directions, respectively and 4 and 8 mm in anterior and posterior directions, respectively (Table2).

Finally, to evaluate the corresponding shifted dose distribution, 18 treatment plans (one for each patient of the cohort) were automatically re-computed using the non-isotropic margins found at 7 min treatment (Table 2) to take into account both the physicians' margin recommendations (24), where a posterior CTV-to-PTV expansion between 3 and 5 mm is needed, and the average duration of an HF treatment (2 min of pre-treatment imaging phase plus 5 min of treatment delivery). Boxplots in Fig.3 report the CTV coverage depending on time. After 5 and 7 min of treatment the prescription constraints on CTV coverage were achieved for 96% of fractions. The same median target coverage as a homogeneous margin of 5 mm was achieved, but with drastically reduced margins in LR, SI and anterior directions.

Discussions

In this study, intrafraction prostate motion was monitored in 46 patients (876 total fractions) that underwent moderate HF radiation therapy, with prostate

monitoring phase ranging between 200 and 600 s. This involved pretreatment imaging and treatment phase. To deliver 3 Gy per fraction in VMAT with flattening filter (FF) photon beams generally takes about 3 min 30 s, whereas delivering hypofractionated treatment of 6 to 7 Gy per fraction generally takes 6 to 7 min. The use of flattening filter free (FFF) beams is likely to divide by 2 the delivery time, thus reducing the probability of prostate motion. Hence, using FFF beams could also lead to a reduction of the treatment margins required compared to FF beams. The large observation time provided in this study enabled us to have a sufficiently large observation period to mimic both moderately and highly hypofractionated treatment delivered with FF or FFF beams.

Similar to other studies, some of which using other monitoring devices, the detected intrafraction displacements were generally small (> 3 mm in 16% of treatment time and > 5 mm in 5% of treatment time) but larger displacements (≥ 8 mm) occurred with a frequency less than 1%, as also reported elsewhere (9, 11, 12, 20). The smallest displacements were observed in LR directions and the largest ones in inferior and posterior directions (7, 9, 11, 17, 25, 26). Hence, even if *Li et al.* (27) showed that the monitoring probe can affect prostate displacements, based on our observations, we can assume that there was no impact of the probe pressure on intrafraction prostate displacement. Possibly, the shift in AP direction was due to a patient relaxation or a change in bladder and rectal fullness. In this direction further research is taking place in our institution to better understand the relationship between the daily anatomical variations and the relative prostate displacements.

Similarly to this work, an increased variance of prostate displacements for longer observation times was found in the literature (9). Generally, using conventional treatment protocols, large target displacements appear to be acceptable if occurring for a short period of time during irradiation. However, during HF treatments such displacements become much more relevant because of the risk of late radiation effects. This makes the calculation of appropriate margins even more important. The analysis of the impact of intrafraction motion on target coverage using homogeneous CTV-to-PTV margins around the CTV showed a general loss in target coverage because of increased treatment times even using up to 6 mm CTV-to-PTV margins. Conversely, analyzing the median shifted dose distribution, for a daily routine HF fraction lasting approximately 5 min, a homogeneous margin of 5 mm should guarantee sufficient target coverage during all treatment.

In the recent literature, there has been a growing interest in finding non-homogeneous minimum margins for considering intrafraction motion as a function of treatment time. A summary of the most recent studies is given in Table 3. In all the studies van Herk's formula was used to calculate time dependent NI-AS margins. An innovative feature of our work is that we compared two different margin calculation strategies over a large cohort of patients. We also

proposed an objective analysis of CTV coverage in function of time using increased CTV-to-PTV margins, without operator dependence, by using an auto planning system to perform the treatment plans.

As a comparison with recent studies, non-isotropic margins were first derived using the van Herk's formula and considering the 90PP-95D dosimetric criterion. The margins obtained in our work were similar in LR and SI directions compared to *Pang et al* (21), considering an observation time of 8 min. Conversely, margin obtained in AP direction was double (5.20 vs 2.65 mm). While after only 4 min of treatment, *Sihono et al.* (11) achieved higher margins in LR direction than other studies, they also found smaller margins in AP direction than in our study (1.33 vs 2.40 mm). *Steiner et al.* (28) obtained the same AP margin of 6.2 mm but after 15 min of observation time versus 10 min for this study.

Therefore, the difference could result in the procedures for patient's preparation before treatment delivery. In our case, the diet suggested to the patients was maybe less respected. In addition, most patients of the cohort were treated between 14-16 pm, which might have a connection with anatomical movements and subsequent prostate movements.

Since prostate displacements observed were more important in posterior and inferior directions, it was relevant to calculate NI-AS margins. Using van Herk's method, margins obtained were smaller than *Pang et al.* (17) in all directions except in posterior direction, after 8 min of treatment. By adapting the dosimetric criteria to HF treatment (95PP-99D), margins were increased by 0.1 mm in left, right and superior directions, 0.2 mm in inferior and anterior directions, and 0.5 mm in posterior direction, after 8 min of treatment. However, van Herk's formula loses accuracy during HF treatments because of the reduced number of fractions (14) and because of non-homogeneous dose distribution. Additionally, patient population cannot be assumed as homogeneous and therefore systematic and random errors are not constant across all population. Systematic errors are also minimized if daily IGRT is performed, which is the case for all SBRT treatments.

By using the voxel shifting method, we made the assumption that the effect of intrafraction motion could be approximated as a shift of the voxel relative to the planning position.

Moreover, considering the asymmetry of prostate movements, this method could be more effective in retrieving NI-AS margins. Considering a 7 min HF treatment (taking also into account the pre-treatment phase), greater margins were found using the voxel shifting method compared to van Herk's margins, except in left and right directions.

Hence, even if the margins found differed between studies, they were all agreed that posterior margins should be more important than in other directions to take into account intrafraction motion. Note that this is contrary to most international protocols which recommend a reduction of the margins in the posterior direction, to reduce the risk of toxicity to the rectum (24).

To validate the robustness of the new CTV-to-PTV margins found with the voxel shifting method, automatic plans were recomputed for a 7 min HF treatment. The evaluation of the dosimetric CTV coverage after 5 and 7 min of treatment was equivalent to the dosimetric coverage obtained with a 5 mm homogeneous margin but with drastically reduced margins in all directions except in posterior.

A possible limitation of our study is that rotations of the prostate were not considered in evaluating non-isotropic margins, as the Clarity 4D TPUS workstation does not support rotations shifts. In the context of our clinical interest in prostate intra-fractional motion, this does not constitute a major drawback.

Finally, similarly to another work, no interplay effect arising from the interaction between intrafraction organ motion and the multileaf collimator position for each particular segment was considered in this study (29). According to the literature, one method to account for this effect consists in using a segment-based convolution method, which involves in convolving the static dose distribution attributed to each segment with the probability density function (PDF) of motion during delivery of the segment (30). Other method consists in using the set of leaf sequences obtained from an electronic portal imaging device to construct the dose distribution (31). Machine log files in combination with Monte Carlo dose calculations have also been widely used (32, 33). Finally, the MR-linac technology allows now combining the linac machine log files with motion information obtained from the intrafraction 3D cine-MR dynamics (34).

Conclusions

To conclude, we reported here our experience in deriving NI-AS duration-dependent margins to generate the required planning target volume for prostate HF radiotherapy treatments. The objective was to propose minimum margin for taking into account intrafraction motion during HF treatment of prostate cancer for centers who do not have the possibility to monitor in real time prostate motion. Similarly to other works, we found that margins should not be reduced in posterior direction, as regularly done in many protocols to minimize the rectal toxicity. Using the voxel shifting method, a 5 mm homogeneous margin was found to be sufficient to ensure a correct CTV dosimetric coverage. NI-AS margin calculation showed that this margin could be reduced in all but

posterior direction.

The use of reduced treatment margins in HF treatment could allow to considerably reduce the dose to the OARs, as shown elsewhere (35). However, to ensure a sufficient CTV coverage without increasing posterior margins, and to minimize the treatment toxicity, a monitoring tool to control prostate's movements seems essential. In our institution, a 5 mm homogeneous CTV-to-PTV margin is used for highly HF prostate treatments. With the results obtained and with the use of the TP-US monitoring modality we should be able to reduce margins to 3 mm. Further work is in progress to assess the dosimetric consequences of these margins on the OARs, as a function of radiotherapy treatment's length.

Acknowledgements

This work was performed within the framework of the SIRIC LYriCAN Grant INCa-INSERM-DGOS-12563, and the LABEX PRIMES(ANR-11-LABX-0063) of Université de Lyon, within the program Investissements d'Avenir (ANR-11-IDEX-0007) operated by the ANR. We are grateful to Sophie King for her involvement in this work.

Conflicts of interest statement

This work was performed in the framework of a research cooperation agreement with Elekta AB.

References

[1] Hegemann NS, Guckenberger M, Belka C, Ganswindt U, Manapov F, Li M. Hypofractionated radiotherapy for prostate cancer. Radiat Oncol 2014;9. https://doi.org/10.1186/s13014-014-0275-6.

[2] Benjamin LC, Tree AC, Dearnaley DP. The Role of Hypofractionated Radiotherapy in Prostate Cancer. Curr Oncol Rep 2017;19:30. https://doi.org/10.1007/s11912-017-0584-7.

[3] Clemente S, Nigro R, Oliviero C, Marchioni C, Esposito M, Giglioli FR, et al. Role of the technical aspects of hypofractionated radiation therapy treatment of prostate cancer: A review. Int J Radiat Oncol Biol Phys 2015;91. https://doi.org/10.1016/j.ijrobp.2014.08.006.

[4] Widmark A, Gunnlaugsson A, Beckman L, Thellenberg-Karlsson C, Hoyer M, Lagerlund M, et al. Ultra-hypofractionated versus conventionally fractionated radiotherapy for prostate cancer: 5-year outcomes of the HYPO-RT-PC randomised, non-inferiority, phase 3 trial. Lancet 2019;394. https://doi.org/10.1016/S0140-6736(19)31131-6.

[5] Litzenberg DW, Balter JM, Hadley SW, Sandler HM, Willoughby TR et al. Influence of intrafraction motion on margins for prostate radiotherapy. Int J Radiat Oncol Biol Phys 2006;65. https://doi.org/10.1016/j.ijrobp.2005.12.033

[6] Chen Z, Yang Z, Wang J, Hu W. Dosimetric impact of different bladder and rectum filling during prostate cancer radiotherapy. Radiat Oncol 2016;11. https://doi.org/10.1186/s13014-016-0681-z.

[7] Li JS, Lin MH, Buyyounouski MK, Horwitz EM, Ma CM. Reduction of prostate intrafractional motion from shortening the treatment time. Phys Med Biol 2013;58. https://doi.org/10.1088/0031-9155/58/14/4921.

[8] Lovelock DM, Messineo AP, Cox BW, Kollmeier MA, Zelefsky MJ. Continuous monitoring and intrafraction target position correction during treatment improves target coverage for patients undergoing sbrt prostate therapy. Int J Radiat Oncol Biol Phys 2015;91. https://doi.org/10.1016/j.ijrobp.2014.10.049.

[9] Langen KM, Willoughby TR, Meeks SL, Santhanam A, Cunningham A, Levine L, et al. Observations on Real-Time Prostate Gland Motion Using Electromagnetic Tracking. Int J Radiat Oncol Biol Phys 2008;71. https://doi.org/10.1016/j.ijrobp.2007.11.054.

[10] Baker M, Behrens CF. Determining intrafractional prostate motion using four dimensional ultrasound system. BMC Cancer 2016;16. https://doi.org/10.1186/s12885-016-2533-5.

[11] Sihono DSK, Ehmann M, Heitmann S, von Swietochowski S, Grimm M, Boda-Heggemann J, et al. Determination of Intrafraction Prostate Motion During External Beam Radiation Therapy With a Transperineal 4-Dimensional Ultrasound Real-Time Tracking System. Int J Radiat Oncol Biol Phys 2018;101. https://doi.org/10.1016/j.ijrobp.2018.01.040.

[12] Richardson AK, Jacobs P. Intrafraction monitoring of prostate motion during radiotherapy using the Clarity® Autoscan Transperineal Ultrasound (TPUS) system. Radiography 2017;23. https://doi.org/10.1016/j.radi.2017.07.003.

[13] de Muinck Keizer DM, Willigenburg T, van der Voort van Zyp JRN, Raaymakers BW, Lagendijk JJW, de Boer JCJ. Prostate intrafraction motion during the preparation and delivery of MR-guided radiotherapy sessions on a 1.5 T MR-Linac. Radiother Oncol 2020;151. https://doi.org/10.1016/j.radonc.2020.06.044.

[14] Herschtal A, Foroudi F, Silva L, Gill S, Kron T. Calculating geometrical margins for hypofractionated radiotherapy. Phys Med Biol 2013;58. https://doi.org/10.1088/0031-9155/58/2/319.

[15] Vanhanen A, Poulsen P, Kapanen M. Dosimetric effect of intrafraction motion and different localization strategies in prostate SBRT. Phys Medica 2020;75. https://doi.org/10.1016/j.ejmp.2020.06.010.

[16] Van Herk M, Remeijer P, Rasch C, Lebesque J V. The probability of correct target dosage: Dose-population histograms for deriving treatment margins in radiotherapy. Int J Radiat Oncol Biol Phys 2000;47. https://doi.org/10.1016/S0360-3016(00)00518-6.

[17] Pang EPP, Knight K, Fan Q, Tan SXF, Ang KW, Master Z, et al. Analysis of intra-fraction prostate motion and derivation of duration-dependent margins for radiotherapy using real-time 4D ultrasound. Phys Imaging Radiat Oncol 2018;5. https://doi.org/10.1016/j.phro.2018.03.008.

[18] Unkelbach J, Alber M, Bangert M, Bokrantz R, Chan TCY, Deasy JO, et al. Robust radiotherapy planning. Phys Med Biol 2018;63. https://doi.org/10.1088/1361-6560/aae659.

[19] Biston MC, Costea M, Gassa F, Serre AA, Voet P, Larson R, et al. Evaluation of fully automated a priori MCO treatment planning in VMAT for head-and-neck cancer. Phys Medica 2021;87. https://doi.org/10.1016/j.ejmp.2021.05.037.

[20] Richter A, Exner F, Weick S, Lawrenz I, Polat B, Flentje M, et al. Evaluation of intrafraction prostate motion tracking using the Clarity Autoscan system for safety margin validation. Z Med Phys 2020;30. https://doi.org/10.1016/j.zemedi.2019.12.004.

[21] Pang EPP, Knight K, Park SY, Lian W, Master Z, Baird M, et al. Duration-dependent margins for prostate radiotherapy—a practical motion mitigation strategy. Strahlentherapie Und Onkol 2020;196. https://doi.org/10.1007/s00066-019-01558-y.

[22] Lachaine M, Falco T. Intrafractional prostate motion management with the Clarity Autoscan system. Med Phys Int 2013;1.

[23] Van Herk M. Errors and Margins in Radiotherapy. Semin Radiat Oncol 2004;14. https://doi.org/10.1053/j.semradonc.2003.10.003.

[24] Brand DH, Tree AC, Ostler P, van der Voet H, Loblaw A, Chu W, et al. Intensity-modulated fractionated radiotherapy versus stereotactic body radiotherapy for prostate cancer (PACE-B): acute toxicity findings from an international, randomised, open-label, phase 3, non-inferiority trial. The Lancet Oncology 2019; 20 https://doi.org/10.1016/S1470-2045(19)30569-8

[25] Xie Y, Djajaputra D, King CR, Hossain S, Ma L, Xing L. Intrafractional Motion of the Prostate During Hypofractionated Radiotherapy. Int J Radiat Oncol Biol Phys 2008;72. https://doi.org/10.1016/j.ijrobp.2008.04.051.

[26] Li JS, Jin L, Pollack A, Horwitz EM, Buyyounouski MK, Price RA, et al. Gains From Real-Time Tracking of Prostate Motion During External Beam Radiation Therapy. Int J Radiat Oncol Biol Phys 2009;75. https://doi.org/10.1016/j.ijrobp.2009.05.022.

[27] Li M, Hegemann N-S, Manapov F, Kolberg A, Thum PD, Ganswindt U, et al. Prefraction displacement and intrafraction drift of the prostate due to perineal ultrasound probe pressure. Strahlentherapie Und Onkol 2017;193. https://doi.org/10.1007/s00066-017-1105-1.

[28] Steiner E, Georg D, Goldner G, Stock M. Prostate and patient intrafraction motion: Impact on treatment time-dependent planning margins for patients with endorectal balloon. Int J Radiat Oncol Biol Phys 2013;86. https://doi.org/10.1016/j.ijrobp.2013.02.035.

[29] Sumida I, Yamaguchi H, Das IJ, Anetai Y, Kizaki H, Aboshi K, et al. Robust plan optimization using edge-enhanced intensity for intrafraction organ deformation in prostate intensity-modulated radiation therapy. Plos one 2017;12(3). https://doi.org/10.1371/journal.pone.0173643.

[30] Li HS, Chetty IJ, Solberg TD. Quantifying the interplay effect in prostate IMRT delivery using a convolution-based method. Med Phys 2008;35. https://doi.org/10.1118/1.2897972.

[31] Lee L, Mao W, Xing L. The use of EPID-measured leaf sequence files for IMRT dose reconstruction in adaptive radiation therapy. Med Phys 2008;35. https://doi.org/10.1118/1.2990782.

[32] Schreibmann E, Dhabaan A, Elder E, Fox T. Patient-specific quality assurance method for VMAT treatment delivery. Med Phys 2009;36. https://doi.org/10.1118/1.3213085.

[33] Litzenberg DW, Hadley SW, Tyagi N, Balter JM, Ten Haken RK, Chetty IJ. Synchronized dynamic dose reconstruction. Med Phys 2007;34. https://doi.org/10.1118/1.2388157.

[34] Kontaxis C, de Muinck Keizer DM, Kerkmeijer LG, Willigenburg T, den Hartogh MD, de Groot-van Breugel EN, et al. Delivered dose quantification in prostate radiotherapy using online 3D cine imaging and treatment log files on a combined 1.5 T magnetic resonance imaging and linear accelerator system. Physics and imaging in radiation oncology 2020; 15. https://doi.org/10.1016/j.phro.2020.06.005.

[35] Zelefsky MJ, Levin EJ, Hunt M, Yamada Y, Shippy AM, Jackson A, et al. Incidence of Late Rectal and Urinary Toxicities After Three-Dimensional Conformal Radiotherapy and Intensity-Modulated Radiotherapy for Localized Prostate Cancer. Int J Radiat Oncol Biol Phys 2008;70. https://doi.org/10.1016/j.ijrobp.2007.11.044.

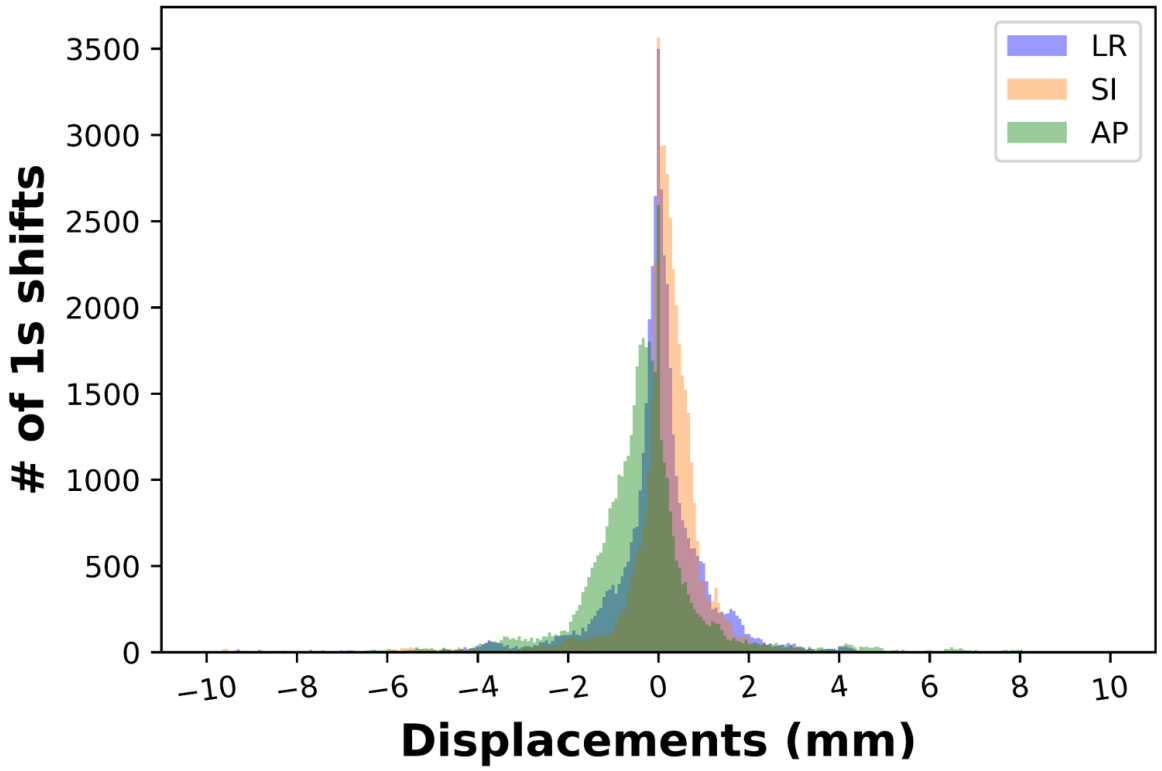

Fig. 1 Distribution of the observed intrafractional prostate displacement for 46 patients (876 sessions)

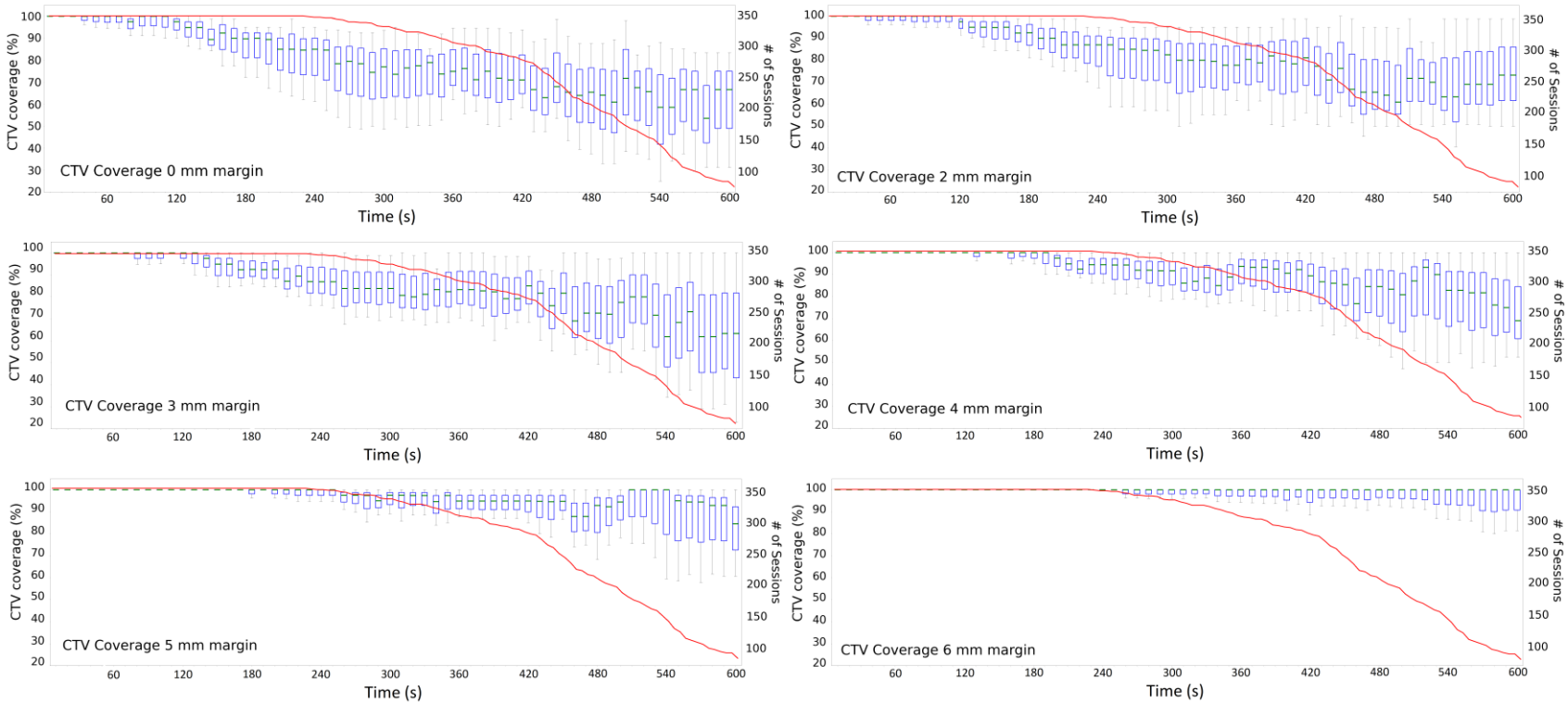

Fig. 2: Boxplot of the CTV coverage in percentage depending on treatment time at 0, 2, 3, 4, 5 and 6 mm margin for 18 patients (346 fractions). Each box is composed of the median CTV coverage (green line), 75 and 25 percentiles values and the total amplitude of the values by the ends of the whiskers. In each figure, the red line represents the number of fractions depending on time. It goes from a maximum of 346 fractions at 0 s to a minimum of 97 fractions at 600s.

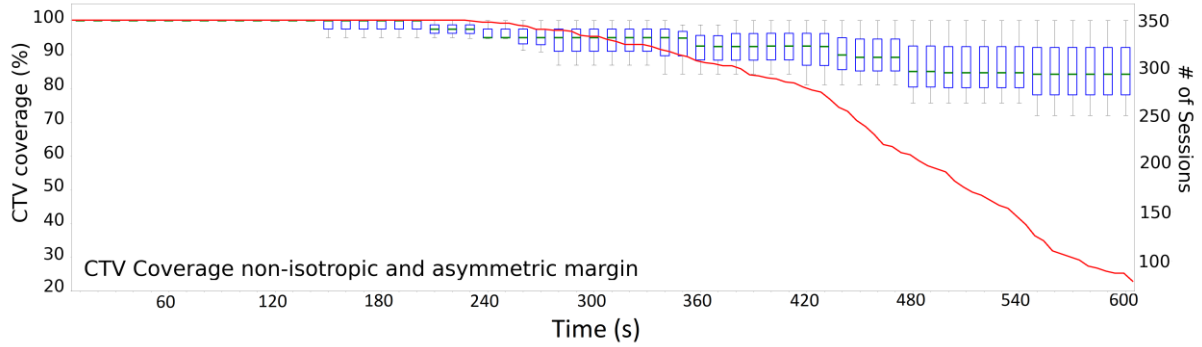

Fig. 3 Boxplot of the CTV coverage in percentage in function of treatment time using non-isotropic margin for 18 patients (346 fractions). Each box is composed of the median CTV coverage (green line), 75 and 25 percentile values and the total amplitude of the values by the ends of the whiskers. The red line represents the number of fractions as a function of time. It goes from a maximum of 346 fractions at 0 s to a minimum of 97 fractions at 600 s.

Table 1: Necessary non-isotropic and asymmetric margins (mm) obtained by van Herk's margin recipe using two different dosimetric criteria. The considered patient population is of 46 patients (876 sessions).

Non-isotropic margins						
	90PP-95D			**95PP-99D**		
Time (min)	**Left-Right**	**Sup- Inf**	**Ant-Post**	**Left-Right**	**Sup- Inf**	**Ant-Post**
1	0.2	0.3	0.6	0.2	0.3	0.6
2	0.3	0.5	1.1	0.3	0.6	1.3
3	0.4	0.9	1.7	0.5	1.0	1.9
4	0.6	1.3	2.4	0.7	1.5	2.8
5	0.7	1.7	3.2	0.9	2.0	3.7
6	0.9	2.1	3.9	1.1	2.4	4.5
7	1.1	2.4	4.5	1.3	2.8	5.3
8	1.2	2.7	5.2	1.4	3.1	6.0
9	1.4	2.9	5.7	1.6	3.4	6.7
10	1.5	3.2	6.2	1.7	3.7	7.2

Non-isotropic and asymmetric margins												
	90PP-95D						**95PP-99D**					
Time (min)	**Left**	**Right**	**Inferior**	**Superior**	**Anterior**	**Posterior**	**Left**	**Right**	**Inferior**	**Superior**	**Anterior**	**Posterior**
1	0.1	0.1	0.1	0.1	0.2	0.2	0.1	0.1	0.1	0.1	0.3	0.3
2	0.1	0.1	0.2	0.2	0.4	0.5	0.1	0.1	0.3	0.3	0.5	0.6
3	0.1	0.2	0.4	0.3	0.5	0.9	0.2	0.2	0.5	0.4	0.6	1.0
4	0.2	0.2	0.6	0.4	0.7	1.3	0.3	0.3	0.7	0.5	0.8	1.5
5	0.3	0.3	0.9	0.5	0.8	1.9	0.3	0.3	1.1	0.6	0.9	2.2
6	0.3	0.4	1.1	0.6	0.9	2.4	0.4	0.4	1.3	0.7	1.0	2.7
7	0.4	0.4	1.3	0.6	0.9	2.8	0.4	0.5	1.5	0.7	1.1	3.2
8	0.4	0.5	1.5	0.7	0.9	3.2	0.5	0.6	1.7	0.8	1.1	3.7
9	0.4	0.5	1.6	0.7	0.9	3.7	0.5	0.6	1.8	0.8	1.1	4.3
10	0.5	0.6	1.7	0.7	0.9	3.5	0.5	0.7	1.9	0.8	1.1	4.6

Table 2: Necessary non-isotropic and asymmetric margins (mm) for meeting 95PP-99D coverage criteria for 46 patients (876 sessions).

Time(min)	Left	Right	Inferior	Superior	Anterior	Posterior
1	0	0	0	0	0	0
2	0	0	0	0	0	2
3	0	0	1	0	1	3
4	0	0	2	0	2	4
5	0	0	2	1	2	5
6	0	0	3	2	3	5
7	0	0	3	2	3	5
8	0	1	3	2	3	6
9	0	1	4	3	4	7
10	0	1	4	3	4	8

Table 3: Comparison between different studies to retrieve asymmetric and non-isotropic CTV-to-PTV margins

Authors	# of patients	Observation time (min)	Margins LR (mm)	Margins SI (mm)	Margins AP (mm)	Notes
Non-isotropic margins						
Pang et al. (23) - 2020	55	8	1.02	2.41	2.65	Prostate monitoring: Clarity 4D TPUS Margins calculation: van Herk's formula
		15	1.84	4.29	4.63	
Sihono et al. (11) - 2018	38	4	1.25	1.10	1.33	Prostate monitoring: Clarity 4D TPUS Margins calculation: van Herk's formula
Steiner et al. (30) - 2013	17	15	2.3	3.9	6.2	Prostate monitoring: Fiducials Margins calculation: Van Herk's formula
di Franco et al. – 2021 (this study)	46	4	0.6	1.3	2.4	Prostate monitoring: Clarity 4D TPUS Margins calculation: van Herk's formula
		8	1.2	2.7	5.2	
		10	1.5	3.2	6.2	
Non-isotropic and asymmetric margins						
Pang et al. (19) - 2018	60	8	0.8 left 0.8 right	1.7 sup 2.7 inf	1.7 ant 2.9 post	Prostate monitoring: Clarity 4D TPUS Margins calculation: van Herk's formula Dosimetric criterion: 90PP – 95D
di Franco et al. – 2021 (this study)	46	8	0.4 left 0.5 right	0.7 sup 1.5 inf	0.9 ant 3.2 post	Prostate monitoring: Clarity 4D TPUS Margins calculation: van Herk's formula Dosimetric criterion: 90PP – 95D
			0.5 left 0.6 right	0.8 sup 1.7 inf	1.1 ant 3.7 post	Prostate monitoring: Clarity 4D TPUS Margins calculation: van Herk's formula Dosimetric criterion: 95PP – 99D
			0 left 1 right	2 sup 3 inf	3 sup 6 inf	Prostate monitoring: Clarity 4D TPUS Margins calculation: voxel shifting Dosimetric criterion: 95PP – 99D